J Pharm Biopharm Res, 2023, 5(1): 349-365
DOI: 10.25082/JPBR.2023.01.001

RESEARCH ARTICLE

Exploring the mechanism of three herb pairs for the treatment of atherosclerosis through network pharmacology and molecular modeling

Minjun Wang

School of Pharmacy, Key Laboratory of Molecular Pharmacology and Drug Evaluation (Yantai University), Ministry of Education, Collaborative Innovation Center of Advanced Drug Delivery System and Biotech Drugs in Universities of Shandong, Yantai University, Yantai, Shandong 264005, China

Correspondence to: Minjun Wang, School of Pharmacy, Yantai University, Yantai, Shandong 264005, China; Email: wangmin4869@126.com

Received: February 3, 2023;
Accepted: April 15, 2023;
Published: April 19, 2023.

Citation: Wang M. Exploring the mechanism of three herb pairs for the treatment of atherosclerosis through network pharmacology and molecular modeling. *J Pharm Biopharm Res*, 2023, **5**(1): 349-365. https://doi.org/10.25082/JPBR.2023.01.001

Abstract: Background: Atherosclerosis (AS) is one of the leading causes of cardiovascular diseases. The traditional China herb pairs such as Huanglian-Gualou, Honghua-Taoren, and Suhexiang-Bingpian showed therapeutic effects on AS by clearing heat and resolving phlegm, invigorating blood and removing blood stasis, as well as aromatic resuscitation, respectively. However, the common and specific mechanisms of these pairs against the same disease are elusive. Objective: This study aimed to explore the molecular mechanisms of 3 herb pairs treating AS by network pharmacology, molecular modeling and mechanism experiments. Methods: The components and their corresponding targets of 3 herb pairs, as well as AS-related targets, were collected from multiple databases and literature. Then the protein-protein interaction network was built to identify the key components and targets associated with AS. The pathway enrichment analysis using KEGG was carried out for analyzing the common mechanisms of 3 herb pairs against AS. Finally, the binding modes of the key components and targets were analyzed by molecular docking and molecular dynamic simulation. Results: The PPI network indicated that the common targets of 3 herb pairs focused on four pathways, including regulated vascular shear stress, TNF, ARE-RAGE, and IL-17 pathways. The molecular docking analysis indicated that the key component quercetin showed highest docking score with PTGS2 in comparison to other targets. Molecular dynamics simulations revealed that quercetin stably anchored to the active pocket of PTGS2 by forming hydrogen bonds with Thr175, Asn351, and Trp356. Conclusion: The molecular mechanism of Huanglian-Gualou, Honghua-Taoren, and Suhexiang-Bingpian against AS was preliminarily expounded, and we wish to provide a theoretical instruction for clinical treatment of AS.

Keywords: atherosclerosis, network pharmacology, molecular docking, molecular dynamics

1 Introduction

Atherosclerosis (AS) is one of the main inducing factors for cardiovascular diseases, including myocardial infarction, heart failure, and stroke. AS also leads to the formation of lipid plaques in the intima of large and medium arteries, accompanied by chronic inflammation. The pathogenesis of AS is complicated, involving abnormal lipid metabolism, inflammatory cell infiltration, uncontrolled immunity, and proliferation of vascular smooth muscle cells (VSMC) [1–3]. Statins are often used to control blood lipid levels in patients for delaying the progression of AS. However, long-term use of statins may cause myocardial function damage [4]. Compared with synthetic drugs, traditional Chinese medicine (TCM) has better biological activities and lower toxicity for treating AS through multiple ways [5]. For example, Huanglian-Gualou and Honghua-Taoren pairs show therapeutic effects on AS by clearing heat and resolving phlegm, invigorating blood and removing blood stasis, respectively. Suhexiang-Bingpian exerts aromatic resuscitation effects against AS.

"Same disease with different treatments" is an essential theory for syndrome differentiation in TCM, which means multiple components of herb or herb pairs exert the synergetic effects against the same disease. For AS, the alkaloids in Huanglian and the triterpenoids in Gualou showed anti-hyperlipidemic and anti-inflammatory activities against AS, respectively (Table 1) [6, 7]. Gualou peel extract reduced the expression of vascular endothelial cell adhesion factor ICAM-1, and inhibited the transformation of monocytes into foam cells [8]. Similarly, the flavonoids and aromatic glycosides in Honghua-Taoren interfered with the process of AS by anticoagulation, inhibiting foam cells formation and proliferation of VSMCs [9, 10]. In contrast, the main components of Suhexiang-Bingpian are volatile oils, which inhibited inflammatory factors and reduce blood viscosity. Therefore, having a better understanding of the molecular

mechanisms of the herb pairs (Huanglian-Gualou, Honghua-Taoren, and Suhexiang-Bingpian) that drive therapeutic effects is of great clinic interest.

Table 1 Effects, formula, and main components of 3 herb pairs

Herb pair	Effect	Formula	Main components
Huanglian-Gualou	Clearing heat and resolving phlegm	XiaoxianXiong Decoction	Alkaloids, triterpenoids
Honghua-Taoren	Invigorating blood and removing blood stasis	XueFuzhuyu Decoction	Flavonoids, aromatic glycosides.
Suhexiang-Bingpian	Aromatic resuscitation	Guanxin suhe Pills	Volatile oils

In this study, a "component-target-pathway" network was built for explaining the therapeutic mechanism of these 3 drug pairs by network pharmacology, and the binding between the hub components and the key targets were analyzed by molecular docking and molecular dynamic simulation. Based on these results, we preliminarily expounded the molecular mechanism of Huanglian-Gualou, Honghua-Taoren, and Suhexiang-Bingpian against AS.

2 Materials and methods

2.1 Collection of active components of 3 herb pairs and AS-related targets

The components and their corresponding targets of six herbs, including alkaloids, triterpenoids, flavonoids, aromatic glycosides, and volatile oils, were retrieved from the TCMSP database (https://old.tcmsp-e.com/tcmsp.php) [11], using "*Rhizoma Coptidis* (Huanglian)", "*Trichosanthes Kirilowii Maxim* (Gualou)", "*Carthami Flos* (Honghua)", "*Persicae Semen* (Taoren)"and "*Borneolum Syntheticum* (Bingpian)" as keywords. Also, the references [12–17] were retrieved to supplement the active components of these 6 herbs. The targets of these components were collected from TCMSP, and predicted using SwissTargetPrediction (http://www.swisstargetprediction.ch) [18] and SEA (https://sea.bkslab.org) [19]. The targets for each component were merged, and the duplicates were removed.The AS-related targets were obtained from OMIM (https://omim.org), DisGeNet (https://www.disgenet.org), and GeneCards (https://www.genecards.org/) using the keyword "AS" [20–22]. After removing the duplicate targets, the remaining ones were used for subsequent study.

2.2 Construction of component-target and protein-protein interaction (PPI) network

The parameters including degree centrality (DC), betweenness centrality (BC), and closeness centrality (CC) are important features for identifying the hub nodes in the network. In this study, a "component-target" network was constructed by Cytoscape 3.8.0 [23], and the degree centrality (DC) was calculated for analyzing the number of targets that each component binds to.Moreover, the intersection of AS-related and the component-related targets of 3 pairs were selected, and one PPI network was constructed by STRING v11.0 (https://cn.string-db.org) [24] with Homo sapiens. After removing the orphaned targets, the targets with confidence scores greater than 0.4 were retained. The targets with more than the median values of three topological features (DC, BC and CC) were considered as the hub targets.

2.3 Kyoto Encyclopedia of genes and genomes (KEGG) enrichment analysis

KEGG (http://www.kegg.jp/) pathway enrichment analysis was performed to analyze the common and specific mechanisms of 3 herb pairs against AS ($p \leq 0.01$).

2.4 Molecular docking

The Surflex-dock module in SYBYL-X 2.1.1 [25] was used to analyze the binding modes between the key components and the targets. The components were optimized using the Tripos force field and Gasteiger-Huckel charges. The crystal structures of four hub targets associated with common mechanisms of 3 herb pairs, including PTGS2 (PDB ID: 4RS0) [26], EGFR (PDB ID: 3POZ) [27], CASP3 (PDB ID: 3DEK) [28], PPARG (PDB ID: 2Q59) [29], were downloaded from the RCSB PDB database (https://www.pdbus.org/). The proteins were pretreated by removing the water molecules, adding hydrogens and charges. The binding site of every target was defined as the pocket of the ligand in the protein, and other parameters required for docking adopted the default values.

2.5 Molecular dynamics simulation

The MD simulation of quercetin and PTGS2 was performed on Gromacs 5.1.4 [30]. The target and the ligand were parameterized with amber99sb-ildnff [31] in Gromacs and GAFF

force field in AMBER 14 [32], respectively. The solvation of the system was constructed with the TIP3P water molecules in a cubic box, and the ions were added to neutralize the system. During MD simulation, the system converged to a minimum energy level using the steepest descent method of 50,000 steps and <10.0 kJ/mol force. Furthermore, one equilibration simulation under constant volume (NVT) using velocity rescaling [33] was conducted with 100 ps, followed by 100 ps with constant pressure (NPT) equilibration using Parrinello-Rahman barostat [34]. Finally, a routine MD simulation for 100 ns was performed without any restraints. Root mean square deviation (RMSD) and root mean square fluctuation (RMSF) of the trajectory were calculated using Gromacs tools. The representative conformation using the GROMOS clustering algorithm was obtained from the dynamically equilibrated MD trajectory.

2.6 Cell culture and determination of NO production

Murine macrophage RAW 264.7 cells were purchased from Cell Bank of the Chinese Academy of Sciences, Shanghai. Then the cells were maintained in RPMI-1640 medium (GIBCO-Life Technologies) with 10% fetal bovine serum (FBS, ExCell Bio). Lipopolysaccharide (LPS) and quercetin was purchased from Solarbio Company, Ltd, and Shanghai Aladdin Reagent Company, Ltd, respectively.

RAW 264.7 cells (5 * 10^4 cells/well) were seeded in 96-well for 24 h. The cells were pre-incubated with quercetin (12.5, 25 and 50 μM, respectively) for 2 h and were then induced with LPS (1 μg/ml) for 24 h. The culture supernatant reacts with Griess reagent for 10 min. Finally, NO production was determined by measuring absorbance at 540 nm using a microplate reader.

3 Results and discussion

3.1 Analysis of PPI network

120 components, including 28 alkaloids in Huanglian and 27 terpenoids in Gualou, 20 flavonoids in Honghua and 11 aromatic glycosides in Taoren, as well as 34 volatile oils in Suhexiang and Bingpian, were collected from the TCMSP database and relevant literature (Table 2). 744 nonredundant targets associated with Huanglian-Gualou, 658 for Honghua-Taoren and 716 for Suhexiang-Bingpian pairs were obtained using TCMSP, SwissTargetPrediction, and SEA databases, respectively (Table 3). Three herb pairs share 98 common targets, which is more than the amount of the unique targets of Huanglian-Gualou (62), Honghua-Taoren (65), and Suhexiang-Bingpian (50). The molecular mechanism of "Same disease with different treatments" were preliminarily proofed by major common targets of 3 herb pairs.

Table 2 Active components of herb pairs

No.	Active components	CAS	Source
MOL1	berberine	2086-83-1	Huanglian
MOL2	berberrubine	17388-19-1	Huanglian
MOL3	Coptisine	3486-66-6	Huanglian
MOL4	palmatine	3486-67-7	Huanglian
MOL5	epiberberine	6873-09-2	Huanglian
MOL6	columbamine	3621-36-1	Huanglian
MOL7	Jatrorrhizine	3621-38-3	Huanglian
MOL8	groenlandicine	38691-95-1	Huanglian
MOL9	Oxyberberine	549-21-3	Huanglian
MOL10	8-Oxoepiberberine	19716-60-0	Huanglian
MOL11	8-Oxycoptisine	19716-61-1	Huanglian
MOL12	8-Oxyberberrubine	29580-82-3	Huanglian
MOL13	sanguinarine	2447-54-3	Huanglian
MOL14	Norsanguinarine	522-30-5	Huanglian
MOL15	Oxysanguinarine	548-30-1	Huanglian
MOL16	Worenine	38763-29-0	Huanglian
MOL17	*(R)*-Canadine	2086-96-6	Huanglian
MOL18	(S)-Canadine	5096-57-1	Huanglian
MOL19	magnoflorine	2141-09-5	Huanglian
MOL20	Chilenine	71700-15-7	Huanglian
MOL21	[1,3]Dioxolo[4,5-g]isoquinolin-5(6H)-one	24188-76-9	Huanglian
MOL22	Noroxyhydrastinine	21796-14-5	Huanglian
MOL23	Corydaldine	493-49-2	Huanglian
MOL24	Thalifoline	21796-15-6	Huanglian
MOL25	ethyl 5-oxoprolinate	66183-71-9	Huanglian
MOL26	Methyl 5-hydroxypyridine-2-carboxylate	30766-12-2	Huanglian
MOL27	Indole-3-carboxaldehyde	487-89-8	Huanglian
MOL28	Choline	62-49-7	Huanglian

MOL29	Karounidiol	118117-31-0	Gualou
MOL30	7-Oxodihydrokarounidiol	143183-47-5	Gualou
MOL31	Multiflorenol	2270-62-4	Gualou
MOL32	Isomultiflorenol	24462-48-4	Gualou
MOL33	Bryonolol	39765-50-9	Gualou
MOL34	Bryonolic acid	24480-44-2	Gualou
MOL35	Cyclokirilodiol	188725-44-2	Gualou
MOL36	Isocyclokirilodiol	188725-45-3	Gualou
MOL37	Cucurbitadienol	35012-08-9	Gualou
MOL38	7-Oxo-10α-cucurbitadienol	155914-81-1	Gualou
MOL39	Arvenin I	65247-27-0	Gualou
MOL40	Cucurbitacin IIa	58546-34-2	Gualou
MOL41	Cucurbitacin B	6199-67-3	Gualou
MOL42	3-Epi-Isocucurbitacin B	89647-62-1	Gualou
MOL43	Isocucurbitacin B	17278-28-3	Gualou
MOL44	Dihydrocucurbitacin B	13201-14-4	Gualou
MOL45	Cucurbitacin D	3877-86-9	Gualou
MOL46	Isocucurbitacin D	68422-20-8	Gualou
MOL47	23,24-Dihydrocucurbitacin D	55903-92-9	Gualou
MOL48	23,24-Dihydrocucurbitacin E	28973-67-3	Gualou
MOL49	(6*R*)-Dehydrovomifoliol	39763-38-7	Gualou
MOL50	Darutigenol	5940-00-1	Gualou
MOL51	β-Sitosterol	83-46-5	Gualou
MOL52	Campesterol	474-62-4	Gualou
MOL53	Daucosterol	474-58-8	Gualou
MOL54	α-Spinasterol	481-18-5	Gualou
MOL55	Stigmasterol	83-48-7	Gualou
MOL56	Carthamin	36338-96-2	Honghua
MOL57	Hydroxysafflor Yellow A	78281-02-4	Honghua
MOL58	quercetin	117-39-5	Honghua
MOL59	Isoquercetin	482-35-9	Honghua
MOL60	Quercimeritrin	491-50-9	Honghua
MOL61	Quercetin 3,7-diglucoside	6892-74-6	Honghua
MOL62	Nicotiflorin	17650-84-9	Honghua
MOL63	Sophoraflavonoloside	19895-95-5	Honghua
MOL64	Apigenin	520-36-5	Honghua
MOL65	Scutellarein	529-53-3	Honghua
MOL66	Rutin	153-18-4	Honghua
MOL67	Kaempferol	520-18-3	Honghua
MOL68	6-Hydroxykaempferol	4324-55-4	Honghua
MOL69	Acacetin	480-44-4	Honghua
MOL70	Kaempferol 7-O-glucoside	16290-07-6	Honghua
MOL71	Luteolin	491-70-3	Honghua
MOL72	Isorhamnetin	480-19-3	Honghua
MOL73	Umbelliferone	93-35-6	Honghua
MOL74	Daphnoretin	2034-69-7	Honghua
MOL75	Myricetin	529-44-2	Honghua
MOL76	Benzyl gentiobioside	56775-64-5	Taoren
MOL77	Amygdalin	29883-15-6	Taoren
MOL78	Vanilloloside	74950-96-2	Taoren
MOL79	Androsin	531-28-2	Taoren
MOL80	Prunasin	99-18-3	Taoren
MOL81	Sambunigrin	99-19-4	Taoren
MOL82	*(R)*-Mandelamide	24008-62-6	Taoren
MOL83	Benzyl β-*D*-Glucopyranoside	4304-12-5	Taoren
MOL84	1-O-(4-Coumaroyl)-β-*D*-glucose	7139-64-2	Taoren
MOL85	Grandidentatin	15732-48-6	Taoren
MOL86	Salireposide	16955-55-8	Taoren
MOL87	Cinnamic acid	140-10-3	Suhexiang
MOL88	Benzoic acid	65-85-0	Suhexiang
MOL89	Benzyl benzoate	120-51-4	Suhexiang
MOL90	Cinnamyl acetate	103-54-8	Suhexiang
MOL91	Methyl cinnamate	103-26-4	Suhexiang
MOL92	Cinnamein	103-41-3	Suhexiang
MOL93	Benzaldehyde	100-52-7	Suhexiang
MOL94	Benzyl acetate	140-11-4	Suhexiang
MOL95	3-Phenylpropanal	104-53-0	Suhexiang
MOL96	Propyl cinnamate	7778-83-8	Suhexiang
MOL97	Cinnamyl cinnamate	122-69-0	Suhexiang
MOL98	Propyl phenylacetate	4606-15-9	Suhexiang
MOL99	vanillin	121-33-5	Suhexiang
MOL100	Cinnamaldehyde	14371-10-9	Suhexiang

MOL101	Bornyl cinnamate 2	41755-67-3	Suhexiang
MOL102	3-Phenylpropionic acid	501-52-0	Suhexiang
MOL103	3-Phenyl-1-propanol	122-97-4	Suhexiang
MOL104	Cinnamyl alcohol	104-54-1	Suhexiang
MOL105	*(-)*-α-Pinene	7785-26-4	Bingpian
MOL106	*(+)*-α-Pinene	7785-70-8	Bingpian
MOL107	1,8-Cineole	470-82-6	Bingpian
MOL108	*(-)*-Isoborneol	124-76-5	Bingpian
MOL109	*(+)*-Isoborneol	16725-71-6	Bingpian
MOL110	*(+)*-Camphene	5794-03-6	Bingpian
MOL111	*(+)*-alpha-Phellandrene	2243-33-6	Bingpian
MOL112	*(-)*-Borneol	464-45-9	Bingpian
MOL113	*(+)*-Borneol	464-43-7	Bingpian
MOL114	*(+)*-alpha-Terpineol	7785-53-7	Bingpian
MOL115	*(+)*-Limonene	5989-27-5	Bingpian
MOL116	*(+)*-3-Carene	498-15-7	Bingpian
MOL117	*(-)*-Camphor	464-48-2	Bingpian
MOL118	*(+)*-Camphor	464-49-3	Bingpian
MOL119	β-Terpineol	138-87-4	Bingpian
MOL120	*(+)*-α-Thujene	563-34-8	Bingpian

Table 3 Related targets of three herb pairs

Huanglian-Gualou	Honghua-Taoren	Suhexing-Bingpian	Huanglian-Gualou	Honghua-Taoren	Suhexing-Bingpian
HTR2B	CA13	PTGS1	SLC18A2	PDK3	DRD2
BCHE	HK2	PTGS2	GSTP1	ERCC5	CNR2
ADRA2C	CXCL12	MAOB	GSTM2	SLC16A3	GPR55
ADRA2B	CA4	MAOA	QTRT1	FEN1	PIK3CB
CHRM1	CA5A	LYZ	CSNK1G1	NR4A2	PIK3CA
ACHE	ALDH1B1	MGAM	CHRNA2	RCE1	CDK5
SIGMAR1	ALDH1A2	F3	RBBP9	LRP6	MAPK14
CYP2D6	AKR1B10	HCAR2	NDUFA4	HNF4A	MAPK11
SAE1	SLC5A2	AKR1B1	PDE1A	MDH1	AURKA
CDC42	CA7	TLR4	FKBP1A	KLK7	TMIGD3
RPS6KB1	CA3	CA2	EDNRA	CA5B	PPP1CA
AURKA	CA6	CA1	DPP4	TAS1R1	HTR6
DHFR	YARS1	ESR2	RAD52	COMT	PDGFRB
RAC1	PTGS1	CA6	AGTR2	RAD51	KDR
AURKB	AR	SLC16A1	PDE1B	ABL1	OPRD1
CYP11B2	PPARG	CA7	PTGDR2	SENP7	OPRK1
GRIA1	PTGS2	CA14	RXRB	NRAS	TNKS
HTR3A	HSP90AA1	CA9	PRKCG	P2RY14	STAT3
GABRB3	PIK3CG	CA5B	HRH2	PCNA	HCRTR2
GABRG2	NCOA2	CA5A	HTR1D	CASP7	KLK8
GABRA5	DPP4	CA12	HTR5A	PTGES	KLK4
IKBKB	AKR1B1	CA4	PRKDC	NUF2	TGM1
CHEK2	PRSS1	CA3	NEK2	ADCY2	USP4
MAP2K1	TOP2A	TRPA1	HAO2	CSNK2A2	SLC7A5
HPGD	F2	ALOX5	CHRNA4	CSNK2B	KLK2
PPIA	KCNH2	MMP9	EGFR	MAPK14	KLK3
SLC1A3	SCN5A	MMP1	PTPRCAP	CCNA2	TGM2
TBXAS1	F10	MMP2	TH	PYGM	F13A1
MAPKAPK2	ADRB2	PTPN1	TSPO	GRIA2	USP5
PRF1	MMP3	AKR1C1	RBP4	OLR1	TGM6
PARP2	PRKACA	AKR1B10	GSK3B	ERN1	EPOR
PIK3CD	F7	CAPN2	PPP5C	NFKB1	PREP
PIK3CB	NOS3	CAPN1	PPARG	TCF4	SLC1A5
PIK3CG	RXRA	IDO1	CCKBR	SHBG	YARS1
ABL1	ACHE	RNPEP	ALOX12	CAMK2A	KCNA2
CHRM4	GABRA1	DAO	RORC	SLC22A3	KYNU
KIT	MAOB	EGFR	PREP	ADRA2B	CASP1
LCK	RELA	NR0B2	FAP	LTA4H	CELA1
SRC	EGFR	GPR183	CASP3	PDGFRB	G6PC
CHEK1	AKT1	SENP2	PGR	FLT4	BMP1
TYMS	VEGFA	CYP1B1	DBF4	TEK	ANPEP
PTGS2	CCND1	RCOR3	ADAMTS5	MAP3K8	KLK5
JAK2	BCL2	PAM	PDGFRA	EPHB4	GRIN2B
CDK2	BCL2L1	CHRNA10	CCR3	FGR	CASP10
CDK4	FOS	CHRNA9	FFAR1	LYN	PPIB
BCAT2	CDKN1A	NFE2L2	TAS2R31	MB	CASP3

EPHB4	EIF6	ESR1	SLC47A1	RNASEH1	PTGER1
TRPC6	BAX	RHOA	CASP8	DAO	CTSS
ICAM1	CASP9	SENP1	CASP1	GSR	CYSLTR1
SELE	PLAU	MYOC	RELA	PTK2B	AMPD3
ALOX5AP	MMP2	NFKB1	NFKBIA	IDO1	CASP9
MAOB	MMP9	HDAC8	CMA1	METAP2	KCNA1
MAPK14	MAPK1	AKR1C3	CTSG	ALDH5A1	SLC16A3
ROCK2	IL10	CES2	FYN	ABAT	RCOR1
LIMK1	EGF	HDAC1	YES1	KCNA3	PPIG
SCN4A	RB1	ABCG2	GLI1	NDUFAB1	MME
PIM1	TNF	PTGER3	NT5E	NDUFAF1	SGMS2
PFKFB3	JUN	TTR	MMP13	NDUFA1	ACE2
F3	IL6	PTGER2	CA4	NDUFA2	SPPL2A
PARP10	CDKN2A	CXCL12	MPO	NDUFA3	P2RX1
HSD17B1	AHSA1	PTGER4	NISCH	NDUFA5	KLK1
MET	CASP3	CES1	KAT2B	NDUFA6	LAP3
CSF1R	TP53	HDAC7	KDM5C	NDUFA7	CAPNS1
RPS27	ELK1	CYP1A1	PTPRC	NDUFA8	FKBP1A
MAPK8	NFKBIA	HDAC2	KDM4B	NDUFA9	GRM3
HCRTR2	POR	HDAC9	ATIC	NDUFA10	LGMN
EPHX2	ODC1	DPYD	PKN2	NDUFA11	ADCYAP1R1
ZAP70	XDH	RBBP9	CA13	NDUFA12	SLC1A1
LYN	CASP8	HDAC11	FPR1	NDUFA13	FFAR1
TEK	TOP1	HDAC6	KDM4C	NDUFB1	CTSV
TRPM8	RAF1	TRPM2	CNR2	NDUFB2	TAB1
PTPN1	SOD1	HDAC5	GRM4	NDUFB3	DPP7
HSD17B2	PRKCA	CHAT	PASK	NDUFB4	KDM1A
CYP11B1	MMP1	FOS	PKIA	NDUFB5	CTRC
FLT3	HIF1A	LPAR2	PDE4B	NDUFB6	CASP4
NTRK1	STAT1	JUN	CES1	NDUFB7	PTPN2
HSD11B1	RUNX1T1	STAT1	CES2	NDUFB8	NAT1
MKNK1	HERC5	TNFRSF1A	NOTUM	NDUFB9	HTT
CDC25B	CDK1	GRIK2	TRPA1	NDUFB10	ADORA1
NOS2	HSPA5	HDAC4	TNKS	NDUFB11	TERT
PTGS1	ERBB2	LPAR3	ST14	NDUFC1	MGLL
KCNH2	ACACA	SLC12A2	GAPDH	NDUFC2	NOS2
ESR1	HMOX1	NR0B1	TYMP	NDUFAF2	MCL1
AR	CYP3A4	HDAC10	AKR1A1	NDUFAF3	ADH4
SCN5A	CYP1A2	AKR1C4	AKR1B10	NDUFAF4	TACR1
F10	CAV1	CYP26B1	TYK2	NDUFS1	TPO
NOS3	MYC	HSPE1	PRMT3	NDUFS2	MPO
RXRA	F3	HSPD1	DPP8	NDUFS3	CHRM4
ADRB2	GJA1	DBH	KDM4A	NDUFS4	CHRNA4
HSP90AA1	CYP1A1	LTB4R	PLAU	NDUFS5	CHRM5
PRKACA	ICAM1	SENP7	PNMT	NDUFS6	CHRNA7
PRSS1	IL1B	NQO1	HMOX1	NDUFS7	PARP1
NCOA2	CCL2	GLO1	PLA2G10	NDUFS8	SLC5A7
PDE10A	SELE	DHFR	MAPKAPK5	NDUFV1	PLK1
CALM1	VCAM1	RELA	RPS6KA4	NDUFV2	CACNA2D1
CYP1B1	PTGER3	TLR9	RPS6KA5	NDUFV3	SRD5A1
CYP1A2	CXCL8	PTPN11	ELANE	MT-ND1	SIGMAR1
RGS17	PRKCB	GNB1	PTP4A3	MT-ND2	SLC18A2
TOP2B	BIRC5	GNG2	MALT1	MT-ND3	CBS
NR0B1	DUOX2	PTPRF	EIF2AK1	MT-ND4L	FDPS
P2RX7	HSPB1	SLC12A5	CSNK1G2	MT-ND5	DAGLA
CA2	TGFB1	GRIK1	CSNK1A1	MT-ND6	AOC3
GABRA1	SULT1E1	TBXAS1	CYP27A1	NDUFA4L2	MIF
GABRA2	MGAM	SENP6	TRPM2	NDUFA4	ALDH2
AKR1B1	IL2	GRM4	S100B	MT-ND4	ERAP2
SLC9A1	NR1I2	HDAC3	FADS1	XPO1	TAS1R1
DRD1	CYP1B1	APP	PLG	DNM2	CASP5
PLK1	CCNB1	KCNQ3	ITGA2B	KCNMA1	MAPK1
PLK3	PLAT	HSPA1A	VEGFA	STS	PSMB1
PLK2	THBD	HTR1E	LDHA	PIM2	FLT3
CFD	SERPINE1	TAAR1	SHBG	RET	PLG
DYRK1A	COL1A1	PIM2	SLC6A5	GCGR	MPI
MAPK10	IFNG	ADH1B	ALDH5A1	WEE1	C1S
PGK1	ALOX5	ADH1C	ABAT	MTOR	CCR1
MCHR1	PTEN	ADH1A	QDPR	PIK3CD	PDE3A
MAPK9	IL1A	PLA2G2E	CXCL12	PIK3CB	PDE4A
NAAA	MPO	PRSS3	HCN4	PIK3CA	PDE2A
ALDH2	NCF1	CHRM3	EP300	PDK1	PDE11A

TTK	HAS2	GABRA2	NFE2L2	ASF1A	CCR5
LTA4H	GSTP1	RXRA	NFKB1	EZR	PDE7B
ABCG2	NFE2L2	GABRA1	GLO1	PDPK1	THRB
ADORA3	NQO1	NCOA2	FOS	FNTA	PIN4
CLK4	PARP1	CA13	CISD1	MMP14	CACNA1D
RAF1	AHR	SRD5A2	DAGLA	VCP	FAAH
MST1R	PSMD3	P4HA1	MMP12	DYRK1A	PPM1B
BMP4	SLC2A4	AKR1C2	DUSP1	ADORA2B	CDC25A
CYP1A1	COL3A1	TAS2R14	IDH1	CLK1	CXCR5
CDK8	CXCL11	CPA3	TLR9	CLK3	GRM6
MDM2	CXCL2	HCAR3	PLEC	DYRK2	S1PR4
TGM2	DCAF5	LPAR5	REN	ROCK1	TRPV1
GRM5	NR1I3	KCNK9	CNR1	DRD1	F2R
GRM1	CHEK2	HIF1AN	TDP2	MMP8	PFKFB3
GCK	INSR	TPMT	PLA2G2C	PNP	TRPM8
MTOR	CLDN4	CYCS	PIN4	TYMS	GABRA3
CTSS	PPARA	RARB	CAD	MAP2K1	ALOX5AP
HSP90AB1	PPARD	KDM3A	HDAC11	PIM3	SREBF2
PRKCB	HSF1	KCNN4	PPM1B	SGK1	PTAFR
MKNK2	CRP	FOLH1	HDAC10	ROCK2	HCRTR1
TGFBR2	CXCL10	RARG	NR1D1	LIMK1	RGS4
SIRT2	CHUK	KDM2A	NPEPPS	CDC42BPA	YWHAG
PDK1	SPP1	PLA2G4B	GLB1	TNK2	ADRA2B
ATR	RUNX2	KDM5C	TAS1R1	DMPK	ADRA1A
IKBKE	RASSF1	PARP10	HSPA1A	NEK1	ADORA2A
KDM5B	E2F1	RXRB	P4HTM	PDE4B	CDK1
TRPV1	E2F2	RARA	NNMT	HDAC6	ADORA2B
TBK1	ACP3	CTRB1	P4HA1	HDAC8	FNTA
SCD	CTSD	KDM4A	MB	HDAC1	QPCT
FGFR3	IGFBP3	KDM4E	FUT7	CDC25A	PIM1
CLK1	IGF2	KDM4C	ALPL	CDC25B	GLP1R
DYRK2	CD40LG	MEP1B	GABRA4	ADAM17	P2RY10
KARS	IRF1	EPHX1	GABRA6	ALPL	GPR174
MARK1	ERBB3	PARP15	KDM3A	FLT1	DNPEP
PDGFRB	PON1	HMGB1	CELA1	FGFR1	GPR34
FPR2	DIO1	CXCL8	LOXL2	CASP6	RPS27
PIM3	PCOLCE	CTBP2	KIF20A	APOBEC3G	CREB1
FLT4	NPEPPS	RXRG	CFTR	SMAD1	GLS
DRD4	NKX3-1	CTSG	AHR	FYN	SCN2A
JAK1	RASA1	DDO	DPYD	STAT3	TAF1L
TUBB	GSTM1	KDM5B	CYP2A6	TH	CYP2D6
SLC22A3	GSTM2	LPAR1	RNASEH1	CD36	KLK6
CYP19A1	NOX4	FUT7	TNFRSF1A	JAK1	AOC2
CD38	AVPR2	SLC6A7	GABRB1	PCK1	FUCA1
NR3C2	MAOA	FEN1	HTR1E	PROC	BAZ2B
PARP1	IGF1R	MITF	TDO2	CDCP1	GABRB2
IMPDH2	FLT3	KMO	ITGB7	ATP1A1	WRN
ROCK1	CYP19A1	SLC22A6	NUAK1	SSTR5	ACE
XBP1	CA2	GSTA1	PSMD14	SSTR2	S1PR5
ADORA2A	PIM1	KDM2B	RAD51	SSTR4	PRNP
PIM2	AURKB	FTO	TPO	SSTR1	RORA
AGPAT2	DRD4	KLF5	CCR1	SSTR3	CACNA1I
SIRT3	ADORA1	SLC15A1	BBOX1	FUCA1	SLC22A1
SIRT1	GLO1	CPA1	SLC5A7	SI	LDHB
GRK5	PIK3R1	KDM5A	NR1H3	FOLH1	PTGES
FLT1	ADORA2A	SLC22A8	VDR	HK1	PPARD
MAP4K4	DAPK1	KCNK3	GLRA1	HPRT1	NPEPPS
EPHA2	PYGL	ERCC5	NR1I3	MMP7	PPID
RPS6KA3	CA1	RPS6KB2	SREBF2	TREH	TMEM97
AXL	GSK3B	KDM4D	CYP17A1	PTAFR	S1PR3
NQO2	SRC	FABP4	CYP51A1	ADA	NOX1
DRD3	PTK2	NR4A1	HMGCR	SQLE	LOXL2
FGFR1	HSD17B2	KDM4B	NR3C1	CDA	RAD51
STAT3	KDR	FABP3	NPC1L1	MGMT	NMBR
UBA2	MMP13	GFER	IGF1R	IGF2R	ALPG
F7	ALOX15	NR1H4	ALK	SLC28A2	PLAA
NCOA1	ABCC1	TDP2	GC	SLC5A11	STK17B
BACE1	PLK1	HNF4A	CD81	MANBA	QDPR
NR1I2	CA12	P4HTM	HSD11B2	SELP	ODC1
KCNMA1	PKN1	SENP8	PTPN2	SELL	KCNB1
PRKAB1	CA14	LIG1	POLB	P2RY6	DNM1
BMPR1A	CA9	KIF11	PRKCH	ADK	DHCR7

ACVRL1	CSNK2A1	RCE1	PTPN11	GBA2	IGF2R
BMPR2	ALOX12	HKDC1	SERPINA6	UGCG	HSD17B3
BMPR1B	MET	PTPsigma	RORA	P2RY4	TRPM5
ACVR1	NEK2	SLC7A11	FNTA	HSPA8	NQO2
MIF	CXCR1	DHODH	PTPN6	CD69	SHBG
RET	CAMK2B	RNASEH1	FDFT1	P2RY2	DUSP3
MMP9	ALK	GABRB1	FABP1	GAPDH	RAF1
MMP1	ABCB1	GPR139	FABP4	PDCD4	CISD1
MCL1	NEK6	APAF1	FABP3	GBA	CAMK2A
WEE1	PLA2G1B	SLC6A1	FABP5	CAPNS1	NOX4
CHRNA7	BACE1	PLAUR	PPARD	P2RX1	SLC22A3
PAK4	AXL	ACP3	PTPRF	NAALAD2	ALOX12
MMP3	ABCG2	NSD2	PLA2G1B	NEU4	KCNMA1
MMP2	NUAK1	ATIC	ACP1	GAA	CCND3
TUBB1	AKR1C2	HAO1	SRD5A2	MAN2B1	PSMD14
DHCR7	AKR1C1	MLYCD	TERT	HEXB	EBP
DRD5	AKR1C3	CTDSP1	PDE4D	HEXA	CHEK1
ESR2	AKR1C4	BHMT	IL6	LYPLA2	PTPN6
CCNA2	AKR1A1	APEX1	G6PD	LYPLA1	ALPI
TOP2A	GPR35	KDM6B	SRD5A1	GLA	ALOX15
CDK3	MAPT	GLRA3	ATP12A	TDP1	IRF3
PLK4	KDM4E	ERN1	TACR1	SLC5A7	NFKBIA
PHLPP2	MYLK	CSNK2A2	TNF	TUBB1	TRPV4
BRAF	SYK	PHGDH	PPARA	CREBBP	TXNRD1
MMP8	APEX1	LTA4H	SLC10A2	OGA	IFNB1
STAT6	PTPRS	PIN1	ADAM17	PDF	ACP1
CLK2	ESR2	ACMSD	GPBAR1	GLB1	POLB
DYRK1B	MPG	ATG4B	PRKCA	PDE4C	MDM2
PSEN2	SLC22A12	CMA1	RASGRP3	TNFRSF1A	PABPC1
OGT	CDK5	PTPRC	MC4R	KLK5	HRH1
MMP26	CCNB3	ESRRG	CXCR3	PLAA	RORC
MMP15	ARG1	PLA2G2D	INCENP	CHIA	RORB
MMP16	CDK6	NCOR1	IL6ST	MCHR1	CHRNB1
TCF4	CDK2	HSP90AA1	PYGL	SRD5A1	CHRNA3
CHRM3	TYR	PLCG1	PYGM	GRK1	CEL
ADRA1B	HSD17B1	ENPEP	HRH1	EPHX2	AVPR2
ADRA1D	ESRRA	NR4A2	CRYAB	AHCY	NR1H3
DRD2	APP	FABP5	SQLE	TYMP	IKBKE
F2	TTR	UCHL1	TOP1	TK1	NR1H2
PIK3CA	MMP12	L3MBTL3	HIF1A	MAPK10	SLC18A3
TGFBR1	CD38	PRMT6	IL1B	DTYMK	MMP12
CDC7	TNKS2	RPA1	PLCG1	KDM4C	SAE1
GAK	TNKS	RBP4	USP7	PIN1	C5AR1
CLK3	TERT	CDC25B	PIN1	AOC3	PGGT1B
SCN9A	ELAVL3	ESRRB	CYP24A1	ADRA1A	ICAM1
EIF2AK3	CYP2C8	EPHX2	POLA1	ACPP	VCAM1
CBFB	ELAVL1	PAX8	LTB4R	GDA	MC4R
ITK	CCR4	DUSP22	PTGER2	HTR3A	DNMT3A
CDK9	CYP2C9	NEU3	PTGER1	KYNU	ECE1
ALOX5	BRAF	CYP2C19	NR1H4	ACER2	CPB2
MAPK3	P4HB	PLEC	PTGER4	CPA3	DPP4
ALDH3A1	CBS	PLA2G1B	SLC22A6	CERT1	DPEP1
MAPK1	CREB1	TYR	GPR55	SLC7A5	FFAR4
PTGES	ANTXR2	ELANE	GPR18	CES2	HMGCR
BACE2	PGF	APOBEC3A	CALCRL	SLC15A1	PTGFR
CSNK1D	AMY1A	HPGDS	AKR1C3	CPN1	GPR17
IRAK4	ST6GAL1	P2RX4	TACR2	CES1	ASAH1
TRHR	CBR1	CARM1	HPGDS	SCN4A	MMP10
ILK	ACP1	CYP1A2	MMP7	KCNN4	PLA2G4A
CA7	KCND3	PTPN7	PGGT1B	SLC18A2	GABRQ
CTSK	SNCA	CCR6	GBA	SLC22A6	CNOT7
GSK3A	NMUR2	CHRM1	NR1H2	TRPM8	MMP8
CA14	RPS6KA3	ADRB1	SHH	PARP10	NAALAD2
CPT1A	ALPI	SLC6A3	UGT2B7	GLS	SLC13A5
ALDH1A1	GSTO1	ADRB2	MSR1	SLC1A1	GGH
ABCB1	QDPR	SLC6A4	EBP	PADI1	FAAH2
RPS6KA1	GRK6	PKIA	PRKCZ	PADI3	THRA
ATP4B	ESR1	TYMS	PTGIR	GPR139	MMP3
FASN	ADRA2C	CRHR1	F2R	C3AR1	OXER1
GPR84	NQO2	F2	ITGAL	PAM	SLCO2A1
ABCC4	ADRA2A	PRSS1	PRKCQ	SLC1A2	MMEL1
ABCC1	PDE5A	PLA2G7	RASGRP1	ANPEP	LPL

BRD7	SLC29A1	PRKCD	MDM4	SLC7A11	ERAP1
ODC1	SLC28A3	CYP11B1	PTGFR	DBH	LY96
SLC22A2	SLC5A1	CXCR2	MPEG1	SLC1A3	GNPAT
SIRT5	CD22	PLA2G2A	GLUL	CPA1	DLG4
EDNRB	FGF1	CYP2A6	AVPR2	PLAUR	GSR
ACVR2B	B4GALT1	ADRA2A	AVPR1A	PABPC1	SLC6A11
PDE5A	HRAS	ADRA2C	OXTR	PADI4	MMP13
PRKCE	FGF2	ALDH3A1	ATP2A1	GRM3	TBXA2R
MGLL	SLC5A4	GABRB3	PPP1CC	ADRB1	CDC25C
LIPG	ERAP1	CYP17A1	PPP2CA	SLC6A3	LTB4R2
ERN1	LGALS9	SQLE	PPP2R5A	LYZ	PHF8
CTSD	ALDH2	RAPGEF4	JUN	CTRB1	CD69
PI4KB	ADORA3	GRM5	PCSK7	PTPN2	BCL2A1
PI4KA	AMY2A	GABRG2	S1PR3	YARS	SIRT5
HDAC6	LGALS4	PIK3CD	S1PR1	GGH	CASP7
OPRM1	LGALS8	CCR8	SLC5A2	CASP2	SCN5A
OPRD1	GJB2	C1R	SLC5A1	P2RX4	PARP3
OPRK1	LGALS3	P2RX7	GLRA2	UMPS	NCEH1
ACACB	MAG	METAP1	LGALS9	SLC37A4	HRH2
IDO1	LGALS7	GABRA5	IL2	RXRG	NPPA
LRRK2	LGALS1	NPY5R	BCL2	PRKCD	S1PR1
ATP4A	HPSE	CTSK	CCNB1	MGLL	ITGA4
ERBB2	CALM1	CTSL	PAX8	HCAR2	FCER2
FAAH	CDK4	CTSB	PTGER3	CHRNA2	ITGB1
JAK3	EEF1E1	TDO2	PTGDR		PLCG2
TRPC3	MDM2	CYP11B2	SLC29A1		EGLN1
PDE3A	BAD	TYMP	SF3B3		ADA
PDE7A	MCL1	AR	SORD		ADAMTS5
XDH	CCND2	LIPE	TYRO3		NCOR2
SLC6A2	IL4	LRRK2	CCNT1		GGPS1
SLC6A3	IKBKG	EGLN3	P2RX3		CYSLTR2
ASF1A	XIAP	NAAA	MERTK		LNPEP
CDK5	CYCS	HTR2A	LIMK2		CYP2C9
DYRK3	CFLAR	HTR2C	CRHR1		MMP14
PTK6	AAGAB	HRH3	MAP3K14		FDFT1
NEK1	INS	HRH4	GRB2		GABBR2
DNM1	FCER2	KIF20A	MME		PTGDR2
HSD17B3	IL13	CYP19A1	AKT2		S1PR2
HDAC1	MS4A2	CHRM2	AKT1		SLC1A2
APP	PSME3	CNR1	AKT3		GABBR1
THRA	G6PC	MAPK8	PRKD1		CYP26A1
THRB	APC	MAPK10	HDAC4		METAP2
ESRRA	TRPM2	DAPK3	EZH2		PLA2G5
ESRRB	SLC5A5	JAK3	MAP3K11		SELL
ALOX15	FXYD2	JAK2	MAP3K9		SHH
CAPN1	ALG5	KCNH2	MAP3K10		EBPL
CXCR2	CFTR	JAK1	TTL		HEXA
CA12	PFKFB3	ALPL	PRKCD		ELOB
CA9	LCK	CDK2	ADCY1		ELOC
GRK6	NAE1	FGFR1	PDE3B		KCNH3
DCK	TBXAS1	DCTPP1	IMPDH1		GRIN1
BAD	BCHE	CDC7	PDE2A		CYP2J2
CYP2C19	HTR2C	HMOX1	PHLPP1		SPHK1
CYP3A4	PLG	SELE	PSEN1		CXCR3
COPS5	CYP2C19	CTSH	CCKAR		TDP1
STAMBP	HSD17B3	HSD11B1	TTPA		NOS3
CA1	CDK5R1	PTK2B	GSTO1		CHRNA2
PDPK1	PDE4D	GCGR	PDCD4		PRODH
KIF11	MIF	TNKS2	CDC25C		CYP51A1
CDK1	ESRRB	HTR2B	IARS		NR1I3
STS	POLI	PDE4B	GSR		GPBAR1
NAMPT	POLH	PDE7A	PLA2G2A		UGT2B7
CDK7	TNNC1	CACNA1B	F2RL1		POLA1
CDC25A	TNNI3	GRIK3	BRD4		NPC1L1
CA5B	TNNT2	SLC9A2	BRD2		G6PD
CA5A	SMAD3	PPARG	ATP1A1		NR3C1
KDR	HSPA1A	SLC37A4	KMT5A		CHRNG
CCNE2	NLRP3	SLC6A5	AOC3		CHRND
SYK	CAT	PPARA	PTAFR		F10
CCNE1	HMGCR	KCNA3	LANCL2		CALM1
CCNB3	C5AR1	ALDH1A1	CDC42BPA		IGHG1
ADORA2B	ITGB2	MTNR1B	DHCR24		GABRA6

VCAM1	TBXA2R	SLC6A2	SLC10A1	ADRA1B
DUSP3	NOS2	MAPT	NPC1	NR3C2
HRH3	HSP90AB1	FABP1	CDC45	TRPV3
GRK2	PGR	PPME1	FGF2	ATP12A
ADK	CHRM1	GFPT1	CD4	CD81
QPCT	GABRA2	ABCB1	ST3GAL1	PGR
NPY5R	SLC6A2	TUBB1	ABCB11	SCD
GLRA3	CHRM2	BCHE	EPHA7	NCOA1
NR4A2	ADRA1B	IKBKG	EPHA5	SERPINA6
TAS2R14	IKBKB	FABP2	EPHA8	VDR
CHRM5	MAPK8	TOP2A	EPHB3	
HTR2A	PPP3CA	NLRP1	EPHA4	
HTR2C	SLPI	ATP6V1B1	EPHA1	
SLC6A4	GNB1	CYP27A1	EPHB1	
ADRA1A	GNG2	CYP24A1	EPHA6	
CHRM2	PTPN1	BACE1	EPHB2	
HTR7	PTPN9	ACHE	EPHB6	
HTR1A	PTPN6	KCNK2	CYP27B1	
HCRTR1	PTPN22	NLRP3	ENPP2	
ADRB3	PTPN13	IMPDH2	EPHA3	
ADRB1	PTPRG	IMPDH1	GBA2	
TBXA2R	DUSP22	HTR5A	GABRA3	
MAOA	NCOA1	MTNR1A	BAX	
MTNR1B	CHEK1	PARP14	CASP9	
CHRNB4	PDE3A	KLKB1	TGFB1	
CHRNA3	FASN	PLAU	PON1	
KCNN3	FASLG	PDGFRA	MAP2	
CHRNB2	KIT	MET	FGF1	
KCNN1	OPRD1	VCP	UGCG	
KCNN2	PLA2G2A	ADORA3	ADH1C	
MTNR1A	SIGMAR1	PDE10A	LYZ	
PPP1CA	KCNA5	TSPO	PRSS3	
CTSL	CDK9	GRM1	TYR	
HTR6	CDK8	PDE5A	SLCO1B1	
ADRA2A	EEF1A1	EP300	ST6GAL1	
BTK	EEF1A2	SNCA	BCL2L1	
ADORA1	PDK4	GRM2	IGHG1	
HTR1B	TAS2R31	HTR1A	CTRB1	

In addition, 1446 AS-related targets were obtained by OMIM, Genecards, and DisGenet, and the PPI networks based on the intersection of component-related targets and AS-related targets were constructed through STRING (Figure 1). The PPI network of AS-related targets and common targets of components identified 4 hub targets with degree > 50, including PTGS2, EGFR, CASP3, and PPARG. PTGS2 (Prostaglandin Endoperoxide Synthase 2, degree = 61) expression induced inflammatory response, and PTGS2 inhibition downregulated the expression of MMPs in macrophages, thus stabilizing atherosclerotic plaque [35]. Flavonoids in Honghua-Taoren, such as quercetin, effectively inhibited PTGS2 for controlling the inflammatory response [36]. EGFR (Epidermal growth factor receptor, degree = 57) inhibition significantly reduced T cell infiltration in the AS process [37], and alkaloids in Huanglian-Gualou reduced the proliferation and migration of VSMCs induced by EGFR [38]. CASP3 (Caspase-3, degree=55) is expressed as an apoptotic protease in atherosclerotic plaques [39], and oxyberberine inhibited the expression of pro-apoptotic protein CASP3 [40]. Moreover, PPARG (Peroxisome proliferator-activated receptor gamma, degree =50) affected lipid metabolism in macrophage foam cells and induced inflammatory response associated with AS [41]. Triterpenoids in Huanglian-Gualou promoted M2 polarization of macrophages for alleviating AS by activating PPARG signal [42].

In addition, we identified 56 hub targets by analyzing the relationship of the AS-related and unique component-related targets. In the Huanglian-Gualou PPI network, MAPK3 has highest degree (degree = 21). Alkaloids and triterpenoids haved been reported to downregulate the expression of the downstream target MMP9 by interacting with MAPK3, and significantly reduced the thickness of carotid intima in mice fed with high cholesterol diet [43]. Oxyberberine reduced the expression of AGEs and RAGE, and regulated the downstream MAPK signal pathway,inhibiting the expression of pro-apoptotic protein CASP3 [40]. Therefore, we hypothesised that the Huanglian-Gualou pair showed clearing heat and resolving phlegm against AS by modulating the MAPK and AGE-RAGE pathways.

In the Honghua-Taoren PPI network, INS and CCL2 exhibit highest degrees (degree = 41 for INS and 34 for CCL2). Flavonoids and aromatic glycosides inhibited the expression of CCL2 in endothelial cells, thereby reducing the lipid infiltration of monocytes [44]. Glycosides also regulated blood lipid levels by inhibiting NF-κB activation, which prevented the transcriptional

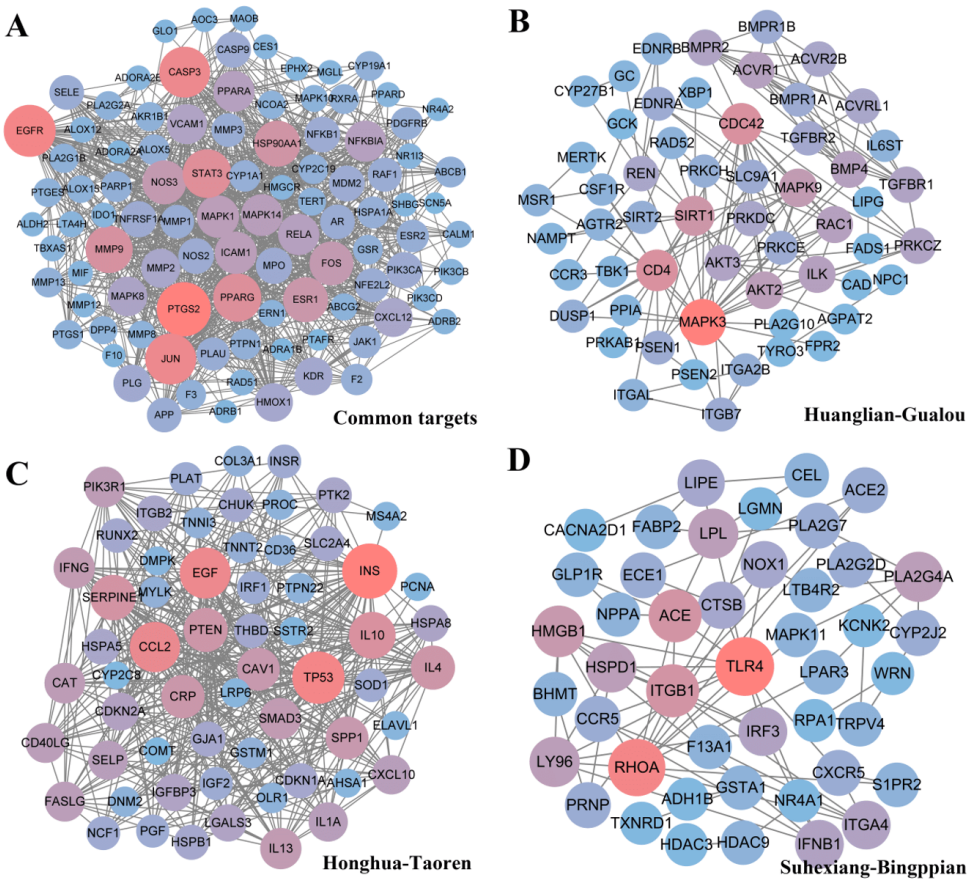

Figure 1 PPI network of disease and component-related targets. AS-related targets with common targets for 3 herb pairs (**A**), unique targets of Huanglian-Gualou (**B**), Honghua-Taoren (**C**) as well as Suhexiang-Bingpian (**D**). The large and red node indicates the node has a high degree value, and the small and blue node manifests the opposite.

expression of PTGS2 and inflammatory factors [45]. Quercetin in Honghua-Taoren has been verfied to alleviate the inflammatory response and endothelial dysfunction caused by insulin resistance [46].

TLR4 is most important in the Suhexiang-Bingpian PPI network (degree = 12). Volatile oils with aromatic resuscitation can improve blood circulation and reduce platelet aggregation [47, 48]. In view of molecular mechanism against AS, volatile oils inhibited TLR4 for reducing the secretion of inflammatory factor PTGS2, and improved the stability of atherosclerotic plaques [49]. Moreover, monoterpenoids in Bingpian also downregulated the expression of TLR4 and p-p65 of NF-κB in vascular endothelial cells for the treatment of AS [50].

3.2 KEGG analysis

Pathway enrichment through KEGG analysis was performed for identifying the common and unique mechanisms of the 3 herb pairs, respectively (Figure 2). The common targets of 3 herb pairs mainly interfered with AS process through five pathways, including fluid shear stress and AS, TNF, AGE-RAGE, IL-17, and apoptosis.

The TNF signaling pathway plays a vital role in regulating inflammation, cell proliferation, and cell death [51]. Activation of TNF receptor induced the degradation of inhibitory protein IKB, leading to chronic inflammation caused by disordered NF-κB transcription [52, 53]. The components of 3 herb pairs showed important therapeutic effects on AS by regulating the TNF pathway. Oxyberberine in Huanglian downregulated the levels of inflammatory factors TNF-α, IL-6, and IL-1β by inhibiting the NF-κB pathway [54]. β-Sitosterol in Gualou and quercetin in Honghua increased the autophagy of macrophages, and inhibited the foaming of macrophages induced by ox-LDL [55, 56]. Aromatic esters and monoterpenoids in Suhexiang-Bingpian inhibited the LPS-induced inflammatory effect of macrophages [57]. Consistent with previous analysis based on the targets, Huanglian-Gualou, Honghua-Taoren, and Suhexiang-Bingpian reversed the endothelial injury mainly through anti-inflammatory and anti-endothelial cell apoptosis.

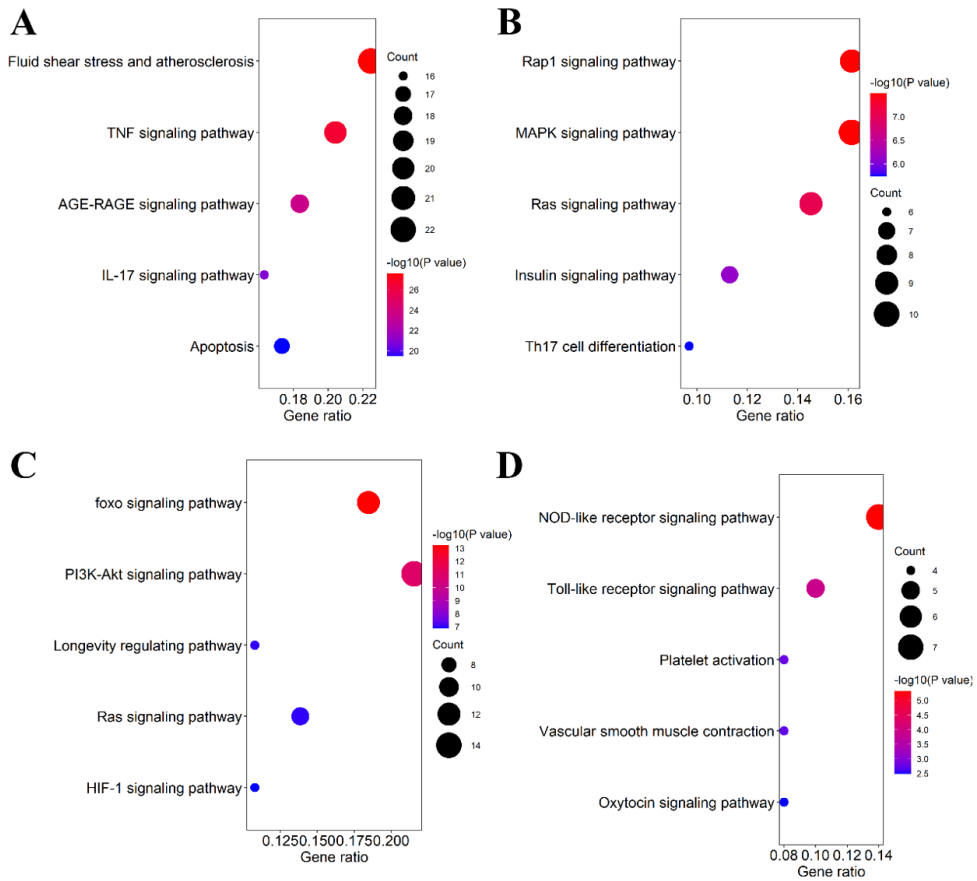

Figure 2 Enriched KEGG pathway of common targets (**A**), and unique targets from Huanglian-Gualou (**B**), Honghua-Taoren (**C**) as well as Suhexiang-Bingpian (**D**)

3.3 Analysis of the key component-related targets

Two components relevant to most hub targets for each herb were considered as key components against AS. Then twelve components for six herbs and their corresponding targets were used to construct a herb-key component-target network (Figure 3). The results showed that flavonoids, including quercetin and apigenin,bind to 232 targets (degree = 232), followed by aryl esters (degree = 147) and triterpenoids, including cinnamein, 3-phenylpropionic acid, β-sitosterol and 7-oxo-10α-cucurbitadienol (degree = 97, Table 4).

Table 4 Degree of key components

Key components	DC	Source
Quercetin	135	Honghua
Apigenin	97	Honghua
3-Phenylpropionic acid	80	Suhexiang
Cinnamein	67	Suhexiang
β-Sitosterol	52	Gualou
7-Oxo-10α-cucurbitadienol	45	Gualou
Oxyberberine	44	Huanglian
(R)-Canadine	42	Huanglian
Benzyl β-*D*-Glucopyranoside	31	Taoren
(+)-α-Terpineol	31	Bingpian
Prunasin	21	Taoren
(+)-Borneol	16	Bingpian

Molecular docking was performed for investigating the binding of 12 key components and top four key targets (PTGS2, EGFR, CASP3, and PPARG). The docking results indicated thatflavonoids, triterpenoids and aromatic glycosides showed good binding abilities with proinflammatory cytokine PTGS2. But volatile oils had poor performance due to their low molecular weights without effectively occupying the active pocket (Figure 4A). Quercetin exhibited best score with proinflammatory cytokine PTGS2 (docking score = 7.82), which is consistent with PTGS inhibition by quercetin for the treatment of AS [58, 59].

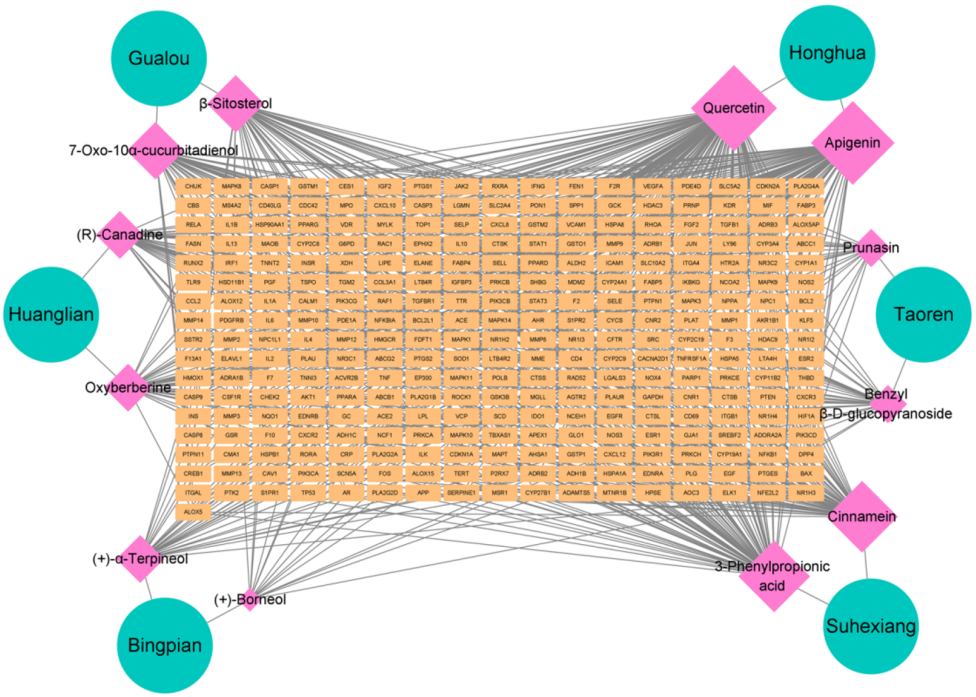

Figure 3 The herb-key component-target Network. Cyan circular, pink diamond and orange rectangular nodes represent herb, key components, and their corresponding targets, respectively.

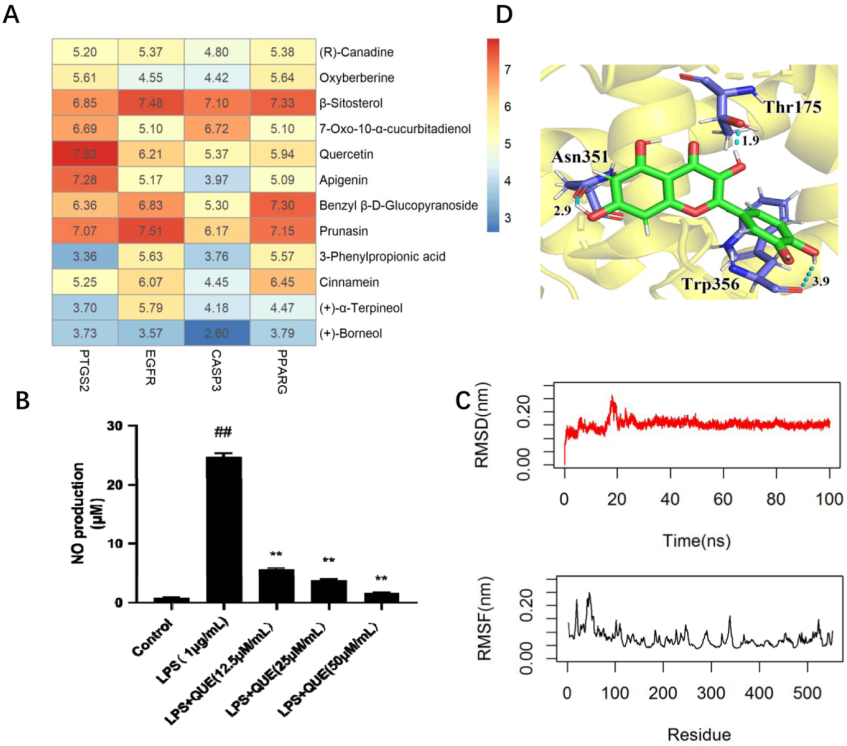

Figure 4 Quercetin negatively regulated NO production in LPS-stimulated RAW264.7 cells by inteacting with PTGS2. . (**A**) Heatmap of molecular docking scores between 12 key components and 4 hub targets. Red indicates a high docking score, and blue does the opposite. (**B**) The effects of quercetin on NO production of RAW264.7. All data are shown as means ± SD; $^{\#\#}p < 0.01$ vs control, and $^{**}p<0.01$ vs model. (**C**) Molecular dynamics (MD) simulation of quercetin and PTGS2. RMSD (red) and RMSF (black) values of PTGS2 are calculated from the backbone after least squares fit to backbone. (**D**) The representative conformation of quercetin bound to PTGS2. The ligand and the target are shown in green and blue sticks, respectively. Hydrogen bonds are shown as cyan dashed lines with labeled distance.

3.4 Molecular dynamics simulation of quercetin bound to PTGS2

Zhu *et al*. reported that NO produced by eNOS reduced the infiltration of inflammatory cells, the expression of chemokines and adhesion factors against AS under normal conditions [60]. In contrast to excessive NO and ROS catalyzed by iNOS caused oxidative stress damage of endothelial cells in inflammatory environment, finally leading to impairment of vascular endothelial function [61]. Consistent with the results of previous studies, we found that quercetin obviously inhibited the release of NO in a dose-dependent manner in LPS-induced macrophages in comparison with the model group (Figure 4B). These results mentioned above verfied that quercetin showed effects on AS by targeting PTGS2. However, the molecular mechanism of ligand-protein binding needs further exploration.

One 100 ns MD simulation was carried out for investigating the stable binding-state of quercetin and PTGS2. The RMSD value of the system showed a stable equilibrium after 27 ns, and the RMSF plot indicated an average atomic fluctuation <0.15 nm for amino acid residues, verifying the conformational stability of ligand-protein complex (Figure 4C). The representative conformation (frame-59200) characterizing 52.3 % conformations in MD clustering analysis with a cutoff of 0.1 nm (Figure 4C) indicated that quertin formed a hydrogen bond network with key residues Thr175, Asn351, and Trp356 of PTGS2 (Figure 4D), which enhanced the stability of the binding between the ligand and the target.

4 Conclusion

In this study, a herb-component-target network was constructed based on 3 herb pairs against AS. Their common mechanism for AS is associated with the inflammatory targets PTGS2, EGFR, CASP3, and PPARG, explaining the molecular mechanism of "Same disease with different treatments". Through cell and modeling experiments, we verified the anti-inflammatory activity of the key component quercetin, and its binding with PTGS2. We wish that our study can provide an theoretical instruction for clinic application of multiple TCMs for the treatment of AS.

Abbreviations

TCM	Traditional Chinese Medicine
AS	Atherosclerosis
PPI	Protein-Protein Interaction
SD	Standard Deviation
VSMC	Vascular Smooth Muscle cells
PTGS2	Prostaglandin-endoperoxide synthase 2
EGFR	Epidermal Growth Factor Receptor
CASP3	Caspase-3
PPARG	Peroxisome Proliferative Activated Receptor Gamma
DC	Degree Centrality
LPS	Lipopolysaccharide

References

[1] Falk E. Pathogenesis of atherosclerosis. Journal of the American College of Cardiology, 2006, **47**: 7-12.
https://doi.org/10.1016/j.jacc.2005.09.068

[2] Gisterå A and Hansson GK. The immunology of atherosclerosis. Nature reviews nephrology, 2017, **13**(6): 368-380.
https://doi.org/10.1038/nrneph.2017.51

[3] Raggi P, Genest J, Giles JT, *et al*. Role of inflammation in the pathogenesis of atherosclerosis and therapeutic interventions. Atherosclerosis, 2018, **276**: 98-108.
https://doi.org/10.1016/j.atherosclerosis.2018.07.014

[4] Okuyama H, Langsjoen PH, Hamazaki T, *et al*. Statins stimulate atherosclerosis and heart failure: pharmacological mechanisms. Expert review of clinical pharmacology, 2015, **8**(2): 189-199.
https://doi.org/10.1586/17512433.2015.1011125

[5] Ting-Ting LI, Zhi-Bin W, Yang LI, *et al*. The mechanisms of traditional Chinese medicine underlying the prevention and treatment of atherosclerosis. Chinese Journal of Natural Medicines, 2019, **17**(6): 401-412.
https://doi.org/10.1016/s1875-5364(19)30048-2

[6] Rui R, Yang H, Liu Y, *et al*. Effects of Berberine on Atherosclerosis. Frontiers in pharmacology, 2021, **12**: 764175.
https://doi.org/10.3389/fphar.2021.764175

[7] Lei X, Li N, Bai Z, *et al*. Chemical constituent from the peel of Trichosanthes kirilowii Maxim and their NF-κB inhibitory activity. Natural Product Research, 2021, **35**(23): 5132-5137.
https://doi.org/10.1080/14786419.2020.1786825

[8] Fu N, Li H, Sun J, *et al*. Trichosanthes pericarpium aqueous extract enhances the mobilization of endothelial progenitor cells and up-regulates the expression of VEGF, eNOS, NO, and MMP-9 in acute myocardial ischemic rats. Frontiers in Physiology, 2018, **8**: 1132.
https://doi.org/10.3389/fphys.2017.01132

[9] Jiagang D, Li C, Wang H, *et al*. Amygdalin mediates relieved atherosclerosis in apolipoprotein E deficient mice through the induction of regulatory T cells. Biochemical and Biophysical Research Communications, 2011, **411**(3): 523-529.
https://doi.org/10.1016/j.bbrc.2011.06.162

[10] Xue X, Deng Y, Wang J, *et al*. Hydroxysafflor yellow A, a natural compound from Carthamus tinctorius L with good effect of alleviating atherosclerosis. Phytomedicine, 2021, **91**: 153694.
https://doi.org/10.1016/j.phymed.2021.153694

[11] Ru J, Li P, Wang J, *et al*. TCMSP: a database of systems pharmacology for drug discovery from herbal medicines. Journal of cheminformatics, 2014, **6**: 1-6.
https://doi.org/10.1186/1758-2946-6-13

[12] Meng FC, Wu ZF, Yin ZQ, *et al*. Coptidis rhizoma and its main bioactive components: recent advances in chemical investigation, quality evaluation and pharmacological activity. Chinese medicine, 2018, **13**: 13.
https://doi.org/10.1186/s13020-018-0171-3

[13] Yu X, Tang L, Wu H, *et al*. Trichosanthis Fructus: botany, traditional uses, phytochemistry and pharmacology. Journal of ethnopharmacology, 2018, **224**: 177-194.
https://doi.org/10.1016/j.jep.2018.05.034

[14] Zhang LL, Tian K, Tang ZH, *et al*. Phytochemistry and Pharmacology of Carthamus tinctorius L. The American journal of Chinese medicine, 2016, **44**(2): 197-226.
https://doi.org/10.1142/s0192415x16500130

[15] Zou L, Zhang Y, Li W, *et al*. Comparison of chemical profiles, anti-inflammatory activity, and UPLC-Q-TOF/MS-based metabolomics in endotoxic fever rats between synthetic borneol and natural borneol. Molecules, 2017, **22**(9): 1446.
https://doi.org/10.3390/molecules22091446

[16] Hovaneissian M, Archier P, Mathe C, *et al*. Analytical investigation of styrax and benzoin balsams by HPLC-PAD-fluorimetry and GC-MS. Phytochemical Analysis, 2008, **19**(4): 301-310.
https://doi.org/10.1002/pca.1048

[17] Tanaka R, Nitta A and Nagatsu A. Application of a quantitative 1 H-NMR method for the determination of amygdalin in Persicae semen, Armeniacae semen, and Mume fructus. Journal of natural medicines, 2014, **68**: 225-230.
https://doi.org/10.1007/s11418-013-0783-y

[18] Gfeller D, Grosdidier A, Wirth M, *et al*. SwissTargetPrediction: a web server for target prediction of bioactive small molecules. Nucleic acids research, 2014, **42**(W1): W32-W38.
https://doi.org/10.1093/nar/gku293

[19] Keiser MJ, Roth BL, Armbruster BN, *et al*. Relating protein pharmacology by ligand chemistry. Nature biotechnology, 2007, **25**(2): 197-206.
https://doi.org/10.1038/nbt1284

[20] Amberger JS, Bocchini CA, Schiettecatte F, *et al*. OMIM. org: Online Mendelian Inheritance in Man (OMIM®), an online catalog of human genes and genetic disorders. Nucleic acids research, 2015, **43**(D1): D789-D798.
https://doi.org/10.1093/nar/gku1205

[21] Piñero J, Bravo À, Queralt-Rosinach N, *et al*. DisGeNET: a comprehensive platform integrating information on human disease-associated genes and variants. Nucleic acids research, 2017, **45**: D833-d839.
https://doi.org/10.1093/nar/gkw943

[22] Rebhan M, Chalifa-Caspi V, Prilusky J, *et al*. GeneCards: integrating information about genes, proteins and diseases. Trends in genetics: TIG, 1997, **13**(4): 163-163.
https://doi.org/10.1016/s0168-9525(97)01103-7

[23] Shannon P, Markiel A, Ozier O, *et al*. Cytoscape: a software environment for integrated models of biomolecular interaction networks. Genome research, 2003, **13**(11): 2498-2504.
https://doi.org/10.1101/gr.1239303

[24] Szklarczyk D, Gable A L, Lyon D, *et al*. STRING v11: protein–protein association networks with increased coverage, supporting functional discovery in genome-wide experimental datasets. Nucleic acids research, 2019, **47**(D1): D607-D613.
https://doi.org/10.1093/nar/gky1131

[25] Louis S. Sybyl.Tripos, Inc. 1699 South Hanley Road, MO 63144-62913.

[26] Lucido MJ, Orlando BJ, Vecchio AJ, *et al*. Crystal structure of aspirin-acetylated human cyclooxygenase-2: insight into the formation of products with reversed stereochemistry. Biochemistry, 2016, **55**(8): 1226-1238.
https://doi.org/10.1021/acs.biochem.5b01378

[27] Aertgeerts K, Skene R, Yano J, *et al*. Structural analysis of the mechanism of inhibition and allosteric activation of the kinase domain of HER2 protein. Journal of Biological Chemistry, 2011, **286**(21): 18756-18765.
https://doi.org/10.1074/jbc.M110.206193

[28] Du JQ, Wu J, Zhang HJ, *et al*. Isoquinoline-1, 3, 4-trione derivatives inactivate caspase-3 by generation of reactive oxygen species. Journal of Biological Chemistry, 2008, **283**(44): 30205-30215.
https://doi.org/10.1074/jbc.M803347200

[29] Bruning JB, Chalmers MJ, Prasad S, *et al*. Partial agonists activate PPARgamma using a helix 12 independent mechanism. Structure (London, England : 1993), 2007, **15**: 1258-1271.
https://doi.org/10.1016/j.str.2007.07.014

[30] Abraham MJ, Murtola T, Schulz R, *et al*. GROMACS: High performance molecular simulations through multi-level parallelism from laptops to supercomputers. SoftwareX, 2015, **1**: 19-25.
https://doi.org/10.1016/j.softx.2015.06.001

[31] Lindorff-Larsen K, Piana S, Palmo K, *et al*. Improved side-chain torsion potentials for the Amber ff99SB protein force field. Proteins: Structure, Function, and Bioinformatics, 2010, **78**(8): 1950-1958.
https://doi.org/10.1002/prot.22711

[32] AMBER14. University of California, San Francisco, 2014.

[33] Bussi G, Donadio D and Parrinello M. Canonical sampling through velocity rescaling. The Journal of chemical physics, 2007, **126**(1): 014101.
https://doi.org/10.1063/1.2408420

[34] Nosé S and Klein ML. Constant pressure molecular dynamics for molecular systems. Molecular Physics, 1983, **50**: 1055-1076.
https://doi.org/10.1080/00268978300102851

[35] Gómez-Hernández A, Martín-Ventura J L, Sánchez-Galán E, *et al*. Overexpression of COX-2, prostaglandin E synthase-1 and prostaglandin E receptors in blood mononuclear cells and plaque of patients with carotid atherosclerosis: regulation by nuclear factor-κB. Atherosclerosis, 2006, 187(1): 139-149.
https://doi.org/10.1016/j.atherosclerosis.2005.08.035

[36] Maleki SJ, Crespo JF annd Cabanillas B. Anti-inflammatory effects of flavonoids. Food chemistry, 2019, **299**: 125124.
https://doi.org/10.1016/j.foodchem.2019.125124

[37] Zeboudj L, Maître M, Guyonnet L, *et al*. Selective EGF-receptor inhibition in CD4+ T cells induces anergy and limits atherosclerosis. Journal of the American College of Cardiology, 2018, **71**(2): 160-172.
https://doi.org/10.1016/j.jacc.2017.10.084

[38] Lee S, Lim HJ, Park HY, *et al*. Berberine inhibits rat vascular smooth muscle cell proliferation and migration in vitro and improves neointima formation after balloon injury in vivo: berberine improves neointima formation in a rat model. Atherosclerosis, 2006, **186**(1): 29-37.
https://doi.org/10.1016/j.atherosclerosis.2005.06.048

[39] Bian W, Jing X, Yang Z, *et al*. Downregulation of LncRNA NORAD promotes Ox-LDL-induced vascular endothelial cell injury and atherosclerosis. Aging (Albany NY), 2020, **12**(7): 6385.
https://doi.org/10.18632/aging.103034

[40] Haftcheshmeh SM, Abedi M, Mashayekhi K, *et al*. Berberine as a natural modulator of inflammatory signaling pathways in the immune system: Focus on NF-κB, JAK/STAT, and MAPK signaling pathways. Phytotherapy Research, 2022, **36**(3): 1216-1230.
https://doi.org/10.1002/ptr.7407

[41] Al-Shali KZ, House AA, Hanley AJG, *et al*. Genetic variation in PPARG encoding peroxisome proliferator-activated receptor γ associated with carotid atherosclerosis. Stroke, 2004, **35**(9): 2036-2040.
https://doi.org/10.1161/01.STR.0000138784.68159.a5

[42] Yang N, Tang Q, Qin W, *et al*. Treatment of obesity-related inflammation with a novel synthetic pentacyclic oleanane triterpenoids via modulation of macrophage polarization. EBioMedicine, 2019, **45**: 473-486.
https://doi.org/10.1016/j.ebiom.2019.06.053

[43] Huang Z, Wang L, Meng S, *et al*. Berberine reduces both MMP-9 and EMMPRIN expression through prevention of p38 pathway activation in PMA-induced macrophages. International journal of cardiology, 2011, **146**(2): 153-158.
https://doi.org/10.1016/j.ijcard.2009.06.023

[44] Hedayati-Moghadam M, Hosseinian S, Paseban M, *et al*. The role of chemokines in cardiovascular diseases and the therapeutic effect of curcumin on CXCL8 and CCL2 as pathological chemokines in atherosclerosis. Natural Products and Human Diseases: Pharmacology, Molecular Targets, and Therapeutic Benefits, 2021, **1328**: 155-170.
https://doi.org/10.1007/978-3-030-73234-9_11

[45] Wang Y, Jia Q, Zhang Y, *et al*. Amygdalin attenuates atherosclerosis and plays an anti-inflammatory role in ApoE knock-out mice and bone marrow-derived macrophages. Frontiers in Pharmacology, 2020, **11**: 590929.
https://doi.org/10.3389/fphar.2020.590929

[46] Guo XD, Zhang DY, Gao XJ, *et al*. Quercetin and quercetin-3-O-glucuronide are equally effective in ameliorating endothelial insulin resistance through inhibition of reactive oxygen species-associated inflammation. Molecular nutrition & food research, 2013, **57**(6): 1037-1045.
https://doi.org/10.1002/mnfr.201200569

[47] Guo J, Qin Z, He Q, *et al*. Shexiang baoxin pill for acute myocardial infarction: Clinical evidence and molecular mechanism of antioxidative stress. Oxidative Medicine and Cellular Longevity, 2021, **2021**: 7644648.
https://doi.org/10.1155/2021/7644648

[48] Wang YH and Zhang YR. Variations in compositions and antioxidant activities of essential oils from leaves of Luodian Blumea balsamifera from different harvest times in China. PLoS One, 2020, **15**(6): e0234661.
https://doi.org/10.1371/journal.pone.0234661

[49] Yang S, Li R, Tang L, *et al*. TLR4-mediated anti-atherosclerosis mechanisms of angiotensin-converting enzyme inhibitor–fosinopril. Cellular immunology, 2013, **285**(1-2): 38-41.
https://doi.org/10.1016/j.cellimm.2013.08.003

[50] Zhang L, Wang F, Zhang Q, *et al*. Anti-inflammatory and anti-apoptotic effects of stybenpropol A on human umbilical vein endothelial cells. International Journal of Molecular Sciences, 2019, **20**(21): 5383.
https://doi.org/10.3390/ijms20215383

[51] Sbarsi I, Falcone C, Boiocchi C, *et al*. Inflammation and atherosclerosis: the role of TNF and TNF receptors polymorphisms in coronary artery disease. International Journal of Immunopathology and Pharmacology, 2007, **20**(1): 145-154.
https://doi.org/10.1177/039463200702000117

[52] Chen G and Goeddel DV. TNF-R1 signaling: a beautiful pathway. Science, 2002, **296**(5573): 1634-1635.
https://doi.org/10.1126/science.1071924

[53] Van Quickelberghe E, De Sutter D, van Loo G, *et al*. A protein-protein interaction map of the TNF-induced NF-κB signal transduction pathway. Scientific data, 2018, **5**(1): 1-9.
https://doi.org/10.1038/sdata.2018.289

[54] Li CL, Tan LH, Wang YF, *et al*. Comparison of anti-inflammatory effects of berberine, and its natural oxidative and reduced derivatives from Rhizoma Coptidis in vitro and in vivo. Phytomedicine, 2019, **52**: 272-283.
https://doi.org/10.1016/j.phymed.2018.09.228

[55] Cao H, Jia Q, Yan L, *et al*. Quercetin suppresses the progression of atherosclerosis by regulating MST1-mediated autophagy in ox-LDL-induced RAW264. 7 macrophage foam cells. International journal of molecular sciences, 2019, **20**(23): 6093.
https://doi.org/10.3390/ijms20236093

[56] Rosenblat M, Volkova N and Aviram M. Pomegranate phytosterol (β-sitosterol) and polyphenolic antioxidant (punicalagin) addition to statin, significantly protected against macrophage foam cells formation. Atherosclerosis, 2013, **226**(1): 110-117.
https://doi.org/10.1016/j.atherosclerosis.2012.10.054

[57] Hao X, Sun W, Ke C, *et al*. Anti-inflammatory activities of leaf oil from Cinnamomum subavenium in vitro and in vivo. BioMed Research International, 2019, **2019**: 1823149.
https://doi.org/10.1155/2019/1823149

[58] Cheng Y, Chu Y, Su X, *et al*. Pharmacokinetic–pharmacodynamic modeling to study the anti-dysmenorrhea effect of Guizhi Fuling capsule on primary dysmenorrhea rats. Phytomedicine, 2018, **48**: 141-151.
https://doi.org/10.1016/j.phymed.2018.04.041

[59] Al-Khayri JM, Sahana GR, Nagella P, *et al*. Flavonoids as potential anti-inflammatory molecules: A review. Molecules, 2022, **27**(9): 2901.
https://doi.org/10.3390/molecules27092901

[60] Zhu Y, Xian X, Wang Z, *et al*. Research progress on the relationship between atherosclerosis and inflammation. Biomolecules, 2018, **8**(3): 80.
https://doi.org/10.3390/biom8030080

[61] Chen J, Ye Z, Wang X, *et al*. Nitric oxide bioavailability dysfunction involves in atherosclerosis. Biomedicine & Pharmacotherapy, 2018, **97**: 423-428.
https://doi.org/10.1016/j.biopha.2017.10.122